Cell shrinkage as a signal to apoptosis in NIH 3T3 fibroblasts

Martin B. Friis, Christel R. Friborg, Linda Schneider, Maj-Britt Nielsen, Ian H. Lambert, Søren T. Christensen and Else K. Hoffmann

Department of Biochemistry, Institute of Molecular Biology and Physiology, The August Krogh Building, University of Copenhagen, Universitetsparken 13, DK-2100 Copenhagen, Denmark

Cell shrinkage is a hallmark of the apoptotic mode of programmed cell death, but it is as yet unclear whether a reduction in cell volume is a primary activation signal of apoptosis. Here we studied the effect of an acute elevation of osmolarity (NaCl or sucrose additions, final osmolarity 687 mosmol l^{-1}) on NIH 3T3 fibroblasts to identify components involved in the signal transduction from shrinkage to apoptosis. After 1.5 h the activity of caspase-3 started to increase followed after 3 h by the appearance of many apoptotic-like bodies. The caspase-3 activity increase was greatly enhanced in cells expressing a constitutively active G protein, Rac ($RacV_{12}A_3$ cell), indicating that Rac acts upstream to caspase-3 activation. The stress-activated protein kinase, p38, was significantly activated by phosphorylation within 30 min after induction of osmotic shrinkage, the phosphorylation being accelerated in fibroblasts overexpressing Rac. Conversely, the activation of the extracellular signal-regulated kinase (Erk1/2) was initially significantly decreased. Subsequent to activation of p38, p53 was activated through serine-15 phosphorylation, and active p53 was translocated from the cytosol to the nucleus. Inhibition of p38 in Rac cells reduced the activation of both p53 and caspase-3. After 60 min in hypertonic medium the rate constants for K^+ and taurine efflux were increased, particular in Rac cells. We suggest the following sequence of events in the cell shrinkage-induced apoptotic response: cellular shrinkage activates Rac, with activation of p38, followed by phosphorylation and nuclear translocation of p53, resulting in permeability increases and caspase-3 activation.

(Received 22 March 2005; accepted after revision 16 June 2005; first published online 23 June 2005)
Corresponding author E. K. Hoffmann: Department of Biochemistry, Institute of Molecular Biology and Physiology, The August Krogh Building, University of Copenhagen, Universitetsparken 13, DK-2100 Copenhagen, Denmark. Email: ekhoffmann@aki.ku.dk

Cell volume homeostasis is crucial for the integrated function of cells, and most animal cells regulate their volume very precisely by mechanisms that have been studied for many years (Hoffmann & Simonsen, 1989; Hoffmann & Dunham, 1995). More recently, it was realized that changes in cell volume may constitute a signal used in basic physiological mechanisms (Lang *et al.* 1998*a*,*b*, 2000*b*). Thus, proliferation and the progress through the cell cycle is frequently associated with cell swelling and with activation of volume regulated anion channels (VRAC) (Nilius, 2001), and is stimulated by osmotic swelling and inhibited by osmotic shrinkage (Anbari & Schultz, 1993; Burg, 2002), whereas cell shrinkage is a hallmark of the early events during programmed cell death by apoptosis (Bortner & Cidlowski, 1998; Maeno *et al.* 2000; Okada *et al.* 2001; Krick *et al.* 2001). Apoptotic cell shrinkage results from a net loss of K^+, Cl^- and organic osmolytes (Best *et al.* 1996; Bortner *et al.* 1997, Lang *et al.* 1998*c*, 2003; Maeno *et al.* 2000; Moran *et al.* 2000), and the causal relationship between ion loss, cell shrinkage and apoptosis is still not well described.

One way to evaluate the effect of cell shrinkage without any concomitant loss of intracellular ions is to examine whether cells enter the mode of apoptosis upon osmotic cell shrinkage. It was recently demonstrated that osmotic shrinkage directly impinge on the apoptotic machinery in a variety of cell types (Roger *et al.* 1999; Qin *et al.* 1999; Moran *et al.* 2000; Terada *et al.* 2001; Burg, 2002; Lang *et al.* 2002) and the effect of osmotic shrinkage seems to be most prominent in cells that are incapable of performing regulatory volume increase (RVI) (Bortner & Cidlowski, 1996). On the other hand, in recent papers Bortner and Cidlowski presented evidence that cell shrinkage can be uncoupled from apoptosis in human lymphoma cells (Bortner & Cidlowski, 2003, 2004).

 DOI: 10.1113/jphysiol.2005.087130

The identity and interplay of signalling pathways during cell shrinkage in both apoptosis and hypertonic stress are poorly understood, although some suggestions have been put forward. Apoptosis and related death modes are highly regulated by mitogen activated protein (MAP) kinases (She *et al.* 2001; Kim *et al.* 2002; Zhu *et al.* 2002), small GTP-binding proteins of the Rho family (Aznar *et al.* 2004), the transcription factor and tumour suppressor protein, p53 (She *et al.* 2001; Kim *et al.* 2002; Zhu *et al.* 2002), and the cysteine protease, caspase-3 (Bortner *et al.* 1997). These signalling components were shown to be affected individually or partly in concert by hypertonic stress in various cell types (Hoffmann & Pedersen, 1998; Roger *et al.* 1999; Maeno *et al.* 2000; Dmitrieva *et al.* 2000, 2001*a*,*b*; Pederson *et al.* 2002; Burg, 2002; De Nadal *et al.* 2002; Shen *et al.* 2002; Reinehr *et al.* 2002). In the renal inner medullar cells it was demonstrated that p53 plays a key role in the balance between cell survival and apoptosis, i.e. p53 protects the cells from hypertonically induced apoptosis at moderate osmolarities (500–600 mosmol l^{-1}) where it causes cell cycle delay, whereas it induces apoptosis at higher osmolarities (700–800 mosmol l^{-1}) (Dmitrieva *et al.* 2000, 2001*a*).

In the present report, we have used NIH 3T3 fibroblasts as a model system to investigate the sequential signalling events leading from cell shrinkage to activation of apoptosis via small G proteins, MAP kinases, p53 and caspase-3. In addition, we tried to correlate these signalling events with an observed secondary change in the cellular permeabilities to potassium and the organic osmolyte, taurine. We here show that overexpression of Rac potentiates shrinkage-induced activation of p38 and caspase-3 as well as increase in cellular permeabilities, and that p38 acts upstream in the activation of p53 and caspase-3.

Methods

Materials

Primary antibodies were from Cell Signalling Technology, Inc. (Beverly, MA, USA): p38 MAP kinase rabbit pAb (no. 9212); phosphor-p38 MAP kinase rabbit pAb (Thr180/Tyr182) (no. 9211); Erk1/2, p44/42 MAP kinase rabbit pAb (no. 9102); phospho-Erk1/2 (Thr202/Tyr204) rabbit pAb (no. 9101); p53 rabbit pAb (no. 9282); p53 mouse mAb (no. 2524), phospho-p53 rabbit pAb sampler kit (no. 9919); phospho-p53 (Ser 15) mouse mAb (no. 9288), cleaved caspase-3 rabbit mAB (no. 9665). Secondary antibodies were from The Jackson Laboratory (Bar Harbor, ME, USA): alkaline phosphatase-conjugated goat antimouse IgG or goat antirabbit IgG, FITC-conjugated goat antimouse IgG and Cy3-conjugated goat antirabbit IgG. p38 inhibitor (Sb203580) was from Sigma-Aldrich (no. S8307).

Cell cultures and media

NIH 3T3 wild-type (wt) and a stable cell line expressing constitutively active Rac 1 ($RacV_{12}A_3$) mouse fibroblasts (Pedersen *et al.* 2002) were cultured in Dulbecco's modified Eagle's medium (DMEM) supplemented with 10% fetal calf serum and 10 ml l^{-1} penicillin–streptomycin, at 37°C, 5% CO_2, 95% humidity. *Hypertonic DMEM* was formed by adding extra NaCl to the desired osmolarities (637–787 mosmol l^{-1}). The potassium concentration in the DMEM was estimated at 5.8 mM. *Isotonic NaCl medium* used in the flux experiments had the following composition: NaCl, 150 mM; Na_2HPO_4, 1 mM; $CaCl_2$, 1 mM; Hepes, 10 mM. *Hypertonic NaCl medium* was identical except for NaCl being 330 mM. *Isotonic Ringer solution* used in the light scatter experiments had the following composition: NaCl, 153 mM; KCl, 6 mM; $MgCl_2$, 1 mM; $CaCl_2$, 1 mM; Hepes, 16.7 mM; glucose, 16.7 mM. *Hypertonic Ringer solution* was identical to the isotonic Ringer solution except for NaCl being 256 mM.

Estimation of cell volume

Cell volume was estimated by light scatter using a Photon Technology International (PTI; Lawrenceville, NJ, USA) RatioMaster spectrophotometer type C-44 as previously described (Pedersen *et al.* 2002). For RVI experiments, cells were incubated in hypertonic Ringer solution solution at 687 mosmol l^{-1}.

Caspase-3 activity assay

Cells were grown to 80% confluency in T75 culture flasks and incubated in either isotonic (337 mosmol l^{-1}) or hypertonic DMEM (637, 687, 737 or 787 mosmol l^{-1}) for 1.5, 3, 4.5 and 6 h. Cells were then trypsinated, transferred to cooled centrifuge tubes with ice-cold DMEM and pelleted by centrifugation at 600 *g* for 5 min at 4°C. Special care was taken to collect all cellular material including apoptotic bodies in the extracellular medium by centrifugation of the culture medium. Cells were lysed in ice-cold lysis buffer (15 mM Hepes (pH 7.4), 2.5 mM CHAPS, 2.5 mM DTT) for 20 min followed by centrifugation at 20 000 *g* to precipitate non-soluble material. The supernatants were transferred to new Eppendorf tubes and protein concentrations were estimated using the Lowry-Petersen-Kaplan method with serum albumin as a standard (Hoffmann *et al.* 1994). Caspase-3 activity in lysates was determined by measuring protease activity using the peptide substrate acetyl-Asp-Glu-Val-Asp *p*-nitroanilide (Ac-DEVD-pNA) as substrate and estimating the *p*-nitroanilide (pNA) production with an assay kit from Sigma-Aldrich (cat. no. 54400) according to the manufacturer's instructions. The results are given as pNa min^{-1} per mg protein.

Test for necrotic cells

The percentage of necrotic cells in cultures subjected to hyperosmotic stress (687 mosmol l^{-1}) for 0, 1.5, 3 and 4.5 h was estimated by staining with propidium iodide, which stains the nuclei in necrotic cells. The assay was performed with the Nucleocounter system (ChemoMetec A/S, DK-3450 Allerød, Denmark) using a nuclei optimization buffer that optimizes the binding of propidium iodide to cell DNA (cat. no. 910-0002) on either whole cells from culture or on cells mixed with a lysis buffer (cat. no. 910-0001). Cells were then sucked into a Nucleocounter Casette (Cat. no. 0502-19) that contains propidium iodide. Counted cells were taken as the total cell number. Subtracting necrotic cells (propidium iodide stained cells) from the total number of cells gave the number of non-necrotic cells. The ratio between non-necrotic cells and the total cell number was then calculated.

Estimation of rate constants

[^{3}H]Taurine and $^{86}Rb^+$ efflux measurements were performed simultaneously as previously described (Pedersen *et al.* 2002). Cells grown to 80% confluence in six-well polyethylene dishes (9.6 cm^2 per well) were loaded for 2 h in DMEM containing [^{3}H] taurine (2135 Bq ml^{-1}) and $^{86}Rb^+$ (40 000 Bq ml^{-1}). The cells were then washed and incubated in hypertonic DMEM medium (687 mosmol l^{-1}) for 60, 90, 120, 150, 180 or 210 min before initiation of the [^{3}H]taurine and $^{86}Rb^+$ efflux experiment. In each case, the efflux experiment was initiated by washing four times with the hypertonic NaCl medium in order to remove extracellular isotope. Hypertonic NaCl medium (1 ml) was added to the dish and the [^{3}H]taurine and $^{86}Rb^+$ efflux subsequently followed for 10 min by removal/addition of 1 ml aliquots of hypertonic solution at 2 min intervals. The cells were lysed at the end of the efflux experiment in NaOH (0.5 mM, 2 h). The aliquots that were removed and the cell lysate plus two washes (double distilled water) were transferred to scintillation vials for estimation of the intracellular $^3H/^{86}Rb^+$ activity (β-scintillation counting, Ultima Gold, PerkinElmer). The total ^{3}H and $^{86}Rb^+$ activity in the cell system was estimated as the sum of activity in all the efflux samples and the intracellular activity. The natural logarithm of the fractions of ^{3}H and $^{86}Rb^+$ activity remaining in the cells at a given time during an efflux experiment was plotted *versus* time for each of the six efflux experiments. The mean rate constants for the taurine efflux and the Rb^+ efflux, within the individual efflux experiment, was subsequently estimated as the negative slope of the graph between the five time points obtained.

Estimation of ion content

Cells grown at 80% confluence in 75 cm^2 flasks were washed three times and incubated for 0, 90, 150 or 210 min in hypertonic NaCl medium (687 mosmol l^{-1}) or alternatively for 270 min in hypertonic DMEM medium. At the end of the incubation period the cells were washed three times with hypertonic sucrose medium (10 mM Hepes supplemented with 200 g sucrose ml^{-1}). The hypertonic solution was aspirated, and the cells lysed in 2 ml of water. Cell lysate (1 ml) was denaturated with 1 ml of NaOH (1 N, overnight) and used for estimation of the protein content by the Lowry method with bovine serum albumin (BSA) as standard. Cell lysate (600 μl) was deproteinized with 50 μl of perchloric acid (70%). K^+ and Na^+ content was estimated by emission flame photometry.

SDS-PAGE and Western blotting analysis

Cells grown to 80% confluence were washed with phosphate-buffered saline (PBS, pH 7.4, 37°C) and incubated for 0, 5, 30, 90 and 180 min in either isotonic (337 mosmol l^{-1}) or hypertonic (687 mosmol l^{-1}) NaCl medium. Cells were then washed quickly in ice-cold PBS and 500 μl of boiling lysis buffer was added (10 mM Tris, pH 7.5, 1% SDS, 1 mM Na_3VO_4). Cell homogenates were scraped off the Petri dishes with a rubber policeman and transferred to 1.5 ml capacity Eppendorf tubes followed by further homogenization with repeated transferring through a 26 gauge needle. The lysates were centrifuged at 16 000 *g* to precipitate non-soluble material. The protein concentration in the supernatants (lysates) was estimated using the Lowry-Petersen-Kaplan method (Hoffmann *et al.* 1994). Lysate samples with 14 μg of protein for MAP kinases and 20–22 μg of protein for p53 were resolved by gel electrophoresis under denaturing and reducing conditions (SDS-PAGE) according to NuPAGE minigel procedures for the NOVEX Xcell (E19001) system (Novex, San Diego, CA, USA). Protein samples for SDS-PAGE were run on 10% NuPAGE bis-tris with NuPAGE Mops SDS running buffer (NP0002). Mark12 standards (Novex) were used as molecular mass markers. Separated proteins were electrophoretically transferred to nitrocellulose membranes using the XCell II Blot Module (Invitrogen). Protein transfer was evaluated by staining the membrane in 1% Ponceau S Red solution (Sigma). The membranes were blocked in milk buffer (5% non-fat dry milk in 1 × TBST (0.01 M Tris-HCl, pH 7.4, 0.15 M NaCl, and 0.1% Tween 20)) for 2 h at room temperature or overnight at 4°C before incubation in blocking buffer with primary antibody for 2 h at room temperature. The membranes were washed once for 15 min and three times for 5 min each in TBST and then incubated with alkaline phosphatase-coupled secondary

antibody for 1 h. The membranes were washed again in TBST and then incubated with a BCIP/NBT solution (Kirkegaard and Perry Laboratories, Gaithersburg, MD, USA). The reactions were stopped by washing in water and air-drying the membranes. The respective antibody dilutions used were 1 : 300 for primary antibodies against MAP kinases and and 1 : 100 for primary antibodies against p53 and cleaved caspase-3. The dilutions used for the secondary antibodies were 1 : 1200 and 1 : 600 for MAP kinases and p53 as well as cleaved caspase-3, respectively.

Immunofluorescence microscopy analysis

Cells grown on conditioned glass coverslips in six-well test plates (Nunc, Roskilde, Denmark) to 80% confluency were washed with PBS and incubated for 30 min in either isotonic (300 mosmol l^{-1}) or hypertonic (687 mosmol l^{-1}) NaCl medium. Cells were then fixed with 4% paraformaldehyde in PBS for 15 min followed by washing in PBS and permeabilization in 0.2% Triton X-100 and 2% BSA in PBS for 10 min. The coverslips were then placed in a moisture chamber and cells were quenched in blocking buffer (2% BSA in PBS) for 30 min followed by incubation with primary antibodies in blocking buffer at room temperature for 2 h. Cells were washed three times for 5 min in PBS and incubated with 4′,6-diamidino-2-phenylindole (DAPI) (Molecular Probes, Leiden, the Netherlands) and secondary antibodies for 1 h followed by washings in PBS. The coverslips were inverted onto a slide containing *ca* 20 μl of mounting medium (70% glycerol, 2% *N*-propylgallate in PBS) and sealed with nail polish. The respective antibody dilutions used were 1 : 50 for primary antibodies for p53 and 1 : 800 for secondary fluorocrom-conjugated goat antimouse antibodies and fluorocrom-conjugated goat antirabbit antibodies.

Statistical analysis

The data are expressed as the means ± s.d. Statistical comparisons were made using an unpaired, two-tailed Student's *t* test with a confidence level of 95%. The significance level was set at $P < 0.05$.

Results

Morphological changes associated with NaCl-induced cell shrinkage

NIH 3T3 cells were incubated in a Ringer solution and shrunk by addition of NaCl to a final osmolarity of 687 mosmol l^{-1}, and changes in cell volume were followed by light scatter. A fast maximum cell shrinkage to ∼0.65 arbitrary units was followed by a slow recovery for the next 1.5 h up to 0.79 arbitrary units, i.e a volume recovery of 40% during 1.5 h (Fig. 1*A*). The recovery rate is always slow but rather variable, and thus the mean volume recovery after 30 min was 29 ± 14% ($n = 6$). The morphological changes associated with high salt treatment for a period up to 330 min is presented in Fig. 1*B*. After 90 min treatment the cells appeared contracted, with few filopodia. Despite the slow volume recovery presented in Fig. 1*A* cells did not regain their normal morphology, but remained in a contracted state that was followed with an increased amount of apoptotic-like cytoplasmic bodies surrounding the cells after 180 min of hypertonic treatment (Fig. 1*B*). It should be noted that data obtained by light scattering in Fig. 1*A* may be affected by these morphological changes.

Shrinkage-induced increase in caspase-3 activity

The cysteine protease, caspase-3, is a key enzyme in the downstream events of the apoptotic process (Maeno *et al.* 2000; Bortner *et al.* 1997; Reinehr *et al.* 2002). In a series of experiments we investigated the activity of caspase-3 in response to cell shrinkage induced by addition of NaCl to the DMEM (hypertonic DMEM). Figure 2*A* shows the caspase-3 activity as a function of extracellular osmolarity 4.5 h after exposure to hypertonic NaCl. A maximal and fivefold increase in caspase-3 activity was observed at 687 mosmol l^{-1}. At higher osmolarities, the activity was less increased. Based on these observations we investigated the time dependence of the caspase-3 activation at 687 mosmol l^{-1}. Figure 2*B* demonstrates a moderate but significant increase from 0.040 ± 0.004 nmol pNA min^{-1} (mg protein)$^{-1}$ ($n = 9$) in isotonic medium to 0.072 ± 0.002 nmol pNA min^{-1} (mg protein)$^{-1}$ ($P < 0.001$, $n = 5$) after 1.5 h and 0.086 ± 0.004 nmol pNA min^{-1} (mg protein)$^{-1}$ ($P < 0.001$, $n = 5$) after 3 h of hypertonic stress. After 4.5 h there was an almost fivefold increase to 0.191 ± 0.024 nmol pNA min^{-1} (mg protein)$^{-1}$ ($n = 9$), which was stable up to 6 h of treatment. Thus, NaCl-induced cell shrinkage is associated with an increase in the activity of caspase-3, which was significant after 1.5 h and amounted to almost fivefold in the period 4.5–6 h at 687 mosmol l^{-1}. At 737 mosmol l^{-1} there was a significant increase in caspase activity after 1.5 h from 0.041 ± 0.003 to 0.079 ± 0.011 nmol pNA min^{-1} mg^{-1} ($P < 0.01$, $n = 7$). At 6 h, the activity decreased to a level below that of the control (0.017 ± 0.017 nmol pNA min^{-1} mg^{-1}). From the results in Fig. 2 we have chosen 687 mosmol l^{-1} for 4.5 h as our standard experimental procedure. Under these conditions there is a high level of caspase-3 activity and no necrotic cell death as estimated by nuclear staining with propidium iodide (Fig. 2*D*).

Importance of the monomeric G protein, rac, for shrinkage-activated caspase-3 activity

To evaluate the role of the monomeric G protein, Rac, in the activation of caspase-3 in hypertonic medium, the experiments shown in Fig. 2*B* were repeated with cells expressing constitutively active Rac (NIH 3T3 $RacV_{12}A_3$). The results are shown in Fig. 2*C*. For comparison, the wild-type result from Fig. 2*B* is included (dashed line). It is seen that the level of caspase-3 activity is increased in

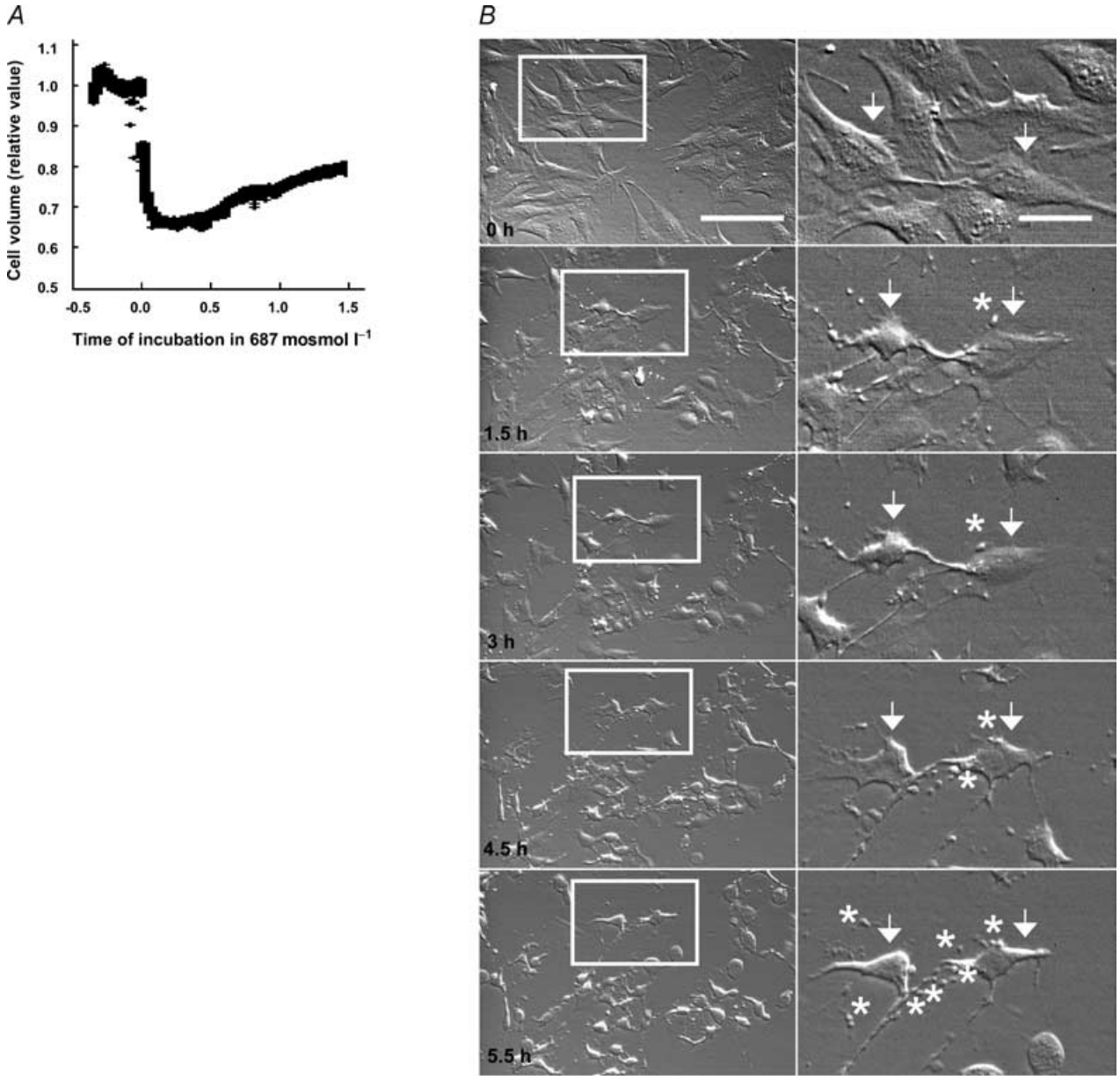

Figure 1. Regulatory volume increase and morphological changes after hypertonic (high NaCl) cell shrinkage

A, cell volume changes in wild-type NIH 3T3 cells as a function of time after hypertonic exposure. Relative cell volume was monitored in adherent NIH 3T3 cells using large angle light scattering. A hypertonic challenge was induced at time zero, by changing the isotonic Ringer perfusion solution to a hypertonic (high NaCl) Ringer solution (687 mosmol l^{-1}). The experiment is representative of six independent experiments lasting up to 30 min and three independent experiments lasting more that 1 h. The mean volume recovery at 30 min was $29 \pm 14\%$ ($n = 6$). *B*, morphology of cells treated with high salt (687 mosmol l^{-1}) added to the DMEM for 0, 1.5, 3, 4.5 and 5.5 h. Scale bar: 100 μm (left row images). The right row of images shows two cells from the left row marked with arrows; notice the cell shrinkage seen at 1.5 h after addition of hypertonic solution. Apoptotic-like cytoplasmatic bodies (marked with asterisks) surrounding the cells were notable after 4.5 and 5.5 h in hypertonic solution. Scale bar: 25 μm.

cells in the hypertonic medium at all time points compared to the isotonic control and that the effect of hypertonicity is more dramatic in $RacV_{12}A_3$ cells compared to that of wild-type cells. In particular, the activity at 4.5 h was increased to 0.568 ± 0.299 nmol pNA min^{-1} (mg protein)$^{-1}$ ($P < 0.05$, $n = 4$), which is an 11-fold increase in activity compared to control cells in isotonic medium and a threefold higher value compared to that obtained with wild-type cells. Thus, Rac is a likely candidate in the signalling cascade between cell shrinkage and caspase-3 activation.

Effect of high extracellular NaCl on the phosphorylation of MAP kinases

The activation of p38 and Erk1/2 during hypertonic (687 mosmol l^{-1}) treatment was investigated in Western blot analysis using antibodies directed against p38 and Erk1/2 (p42/p44) in their non-phosphorylated and phosphorylated (phospho-p38 and phospho-Erk1/2) forms. The phosphorylation level of Erk1/2 dramatically decreased after 5 min in hypertonic medium compared with the isotonic control (Fig. 3) This was followed by

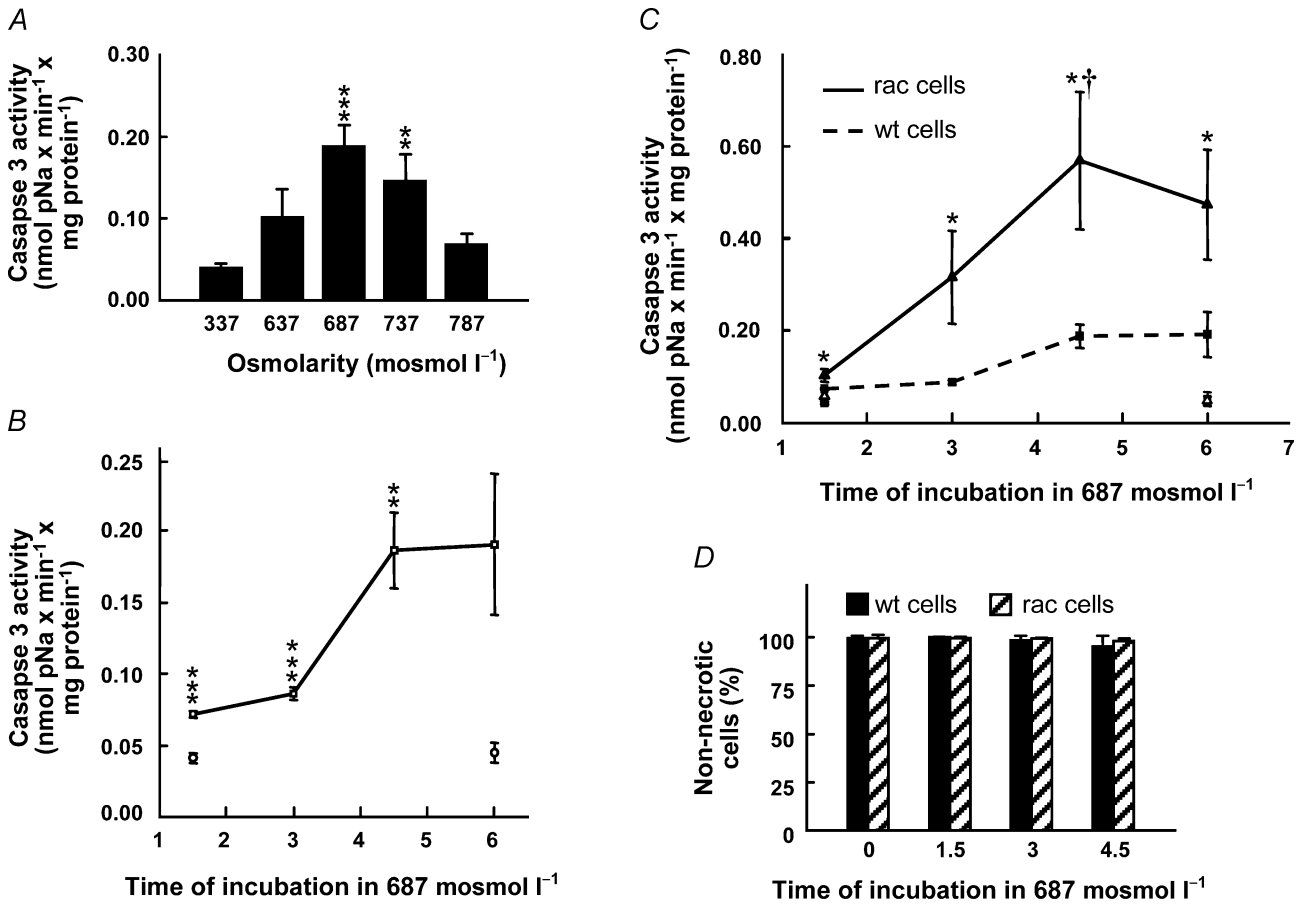

Figure 2. Caspase-3 activity as a function of increasing osmolarity and incubation time in NIH 3T3 cells and $RacV_{12}A_3$ cells

A, cells were incubated in either isotonic (337 mosmol l^{-1}) or hypertonic (high NaCl) DMEM (637, 687 or 787 mosmol l^{-1}) for 4.5 h. The number (*n*) of independent experiments was ≥ 3. *B*, cells were incubated at either 337 mosmol l^{-1} (○) or 687 mosmol l^{-1} (□) for 1.5, 3, 4.5 and 6 h. The number (*n*) of independent experiments was ≥ 3. *C*, cells were incubated in either isotonic (337 mosmol l^{-1}) or hypertonic (687 mosmol l^{-1}) DMEM for 1.5, 3, 4.5 and 6 h. Symbols: □, isotonic NIH 3T3 cells; △, isotonic $RacV_{12}A_3$ cells; ■, hypertonic NIH 3T3 cells; ▲, hypertonic $RacV_{12}A_3$ cells. The number of independent experiments was ≥ 4.The cells were in all cases lysed, and cell lysate was incubated with the colorimetric caspase-3 substrate, Ac-DEVD-pNA, and quantified at 405 nm. The error bars indicate standard error of the mean. $^*P < 0.05$, $^{**}P < 0.01$, $^{***}P < 0.001$, significantly different from the isotonic control. †$P < 0.05$, significantly different from the wt cells at the same time point. *D*, test for necrosis. NIH 3T3 cells (wt) or RacV12A3 cells (rac) were incubated in either isotonic (337 mosmol l^{-1}) DMEM or in hypertonic (high NaCl) DMEM (687 mosmol l^{-1}) for 1.5, 3 and 4.5 h. The number of cells with an intact membrane (cells that are not necrotic) was evaluated using propidium iodide staining. The number (*n*) of independent experiments was 2 for wt and 3 for rac cells.

a gradual equalization of the phosphorylation level of Erk1/2 in isotonic and hypertonic treated cells during the following 3 h (Fig. 3). Note that the isotonic control after 5 min increased when a shift in medium was introduced by a respiration/readdition of medium (Fig. 3*A*) which in itself represents a significant sheer stress. We thus repeated the experiments by adding NaCl (or vehicle) directly to the cells without a change of the medium. As seen in Fig. 3*C* and *D* the phosphorylation level of Erk1/2 remained essentially constant in isotonic medium under this condition whereas it decreased dramatically at 5 min under the hypertonic (high salt) condition.

p38 was significantly phosphorylated after 30 min in hypertonic medium compared to the isotonic control (Fig. 4*A* and *B*) and this phosphorylation level was further increased to about eightfold at 180 min. The level of p38 was constant during this period (Fig. 4*A*). To exclude an involvement of salt stress in hypertonicity-induced changes in p38 phosphorylation, we show that p38 was phosphorylated by sucrose (687 mosmol l^{-1}) at a level comparable to that induced by salt after 30 min of hypertonic treatment (inset in Fig. 4*B*).

The Importance of the monomeric G protein Rac for shrinkage-activated p38

To evaluate the role of the monomeric G protein Rac in the activation of p38 in hypertonic medium, the experiments shown in Fig. 4*A* and *B* were repeated with cells expressing constitutively active Rac (NIH 3T3 $RacV_{12}A_3$). The results presented in Fig. 4*C* and *D* show that p38 phosphorylation was accelerated in Rac cells, i.e. it was already significant after 5 min, indicating that cell shrinkage-induced activation of p38 proceeds via an activation of Rac.

Effect of cell shrinkage on the phosphorylation and nuclear translocation of p53

The multifunctional transcription factor and tumour suppressor protein p53 has numerous N-terminal amino acid motifs that upon phosphorylation activate the protein by structural modifications. Upon phosphorylation, p53 translocates to the nucleus where it serves as an activator of apoptosis. The activation of p53 in hypertonic medium

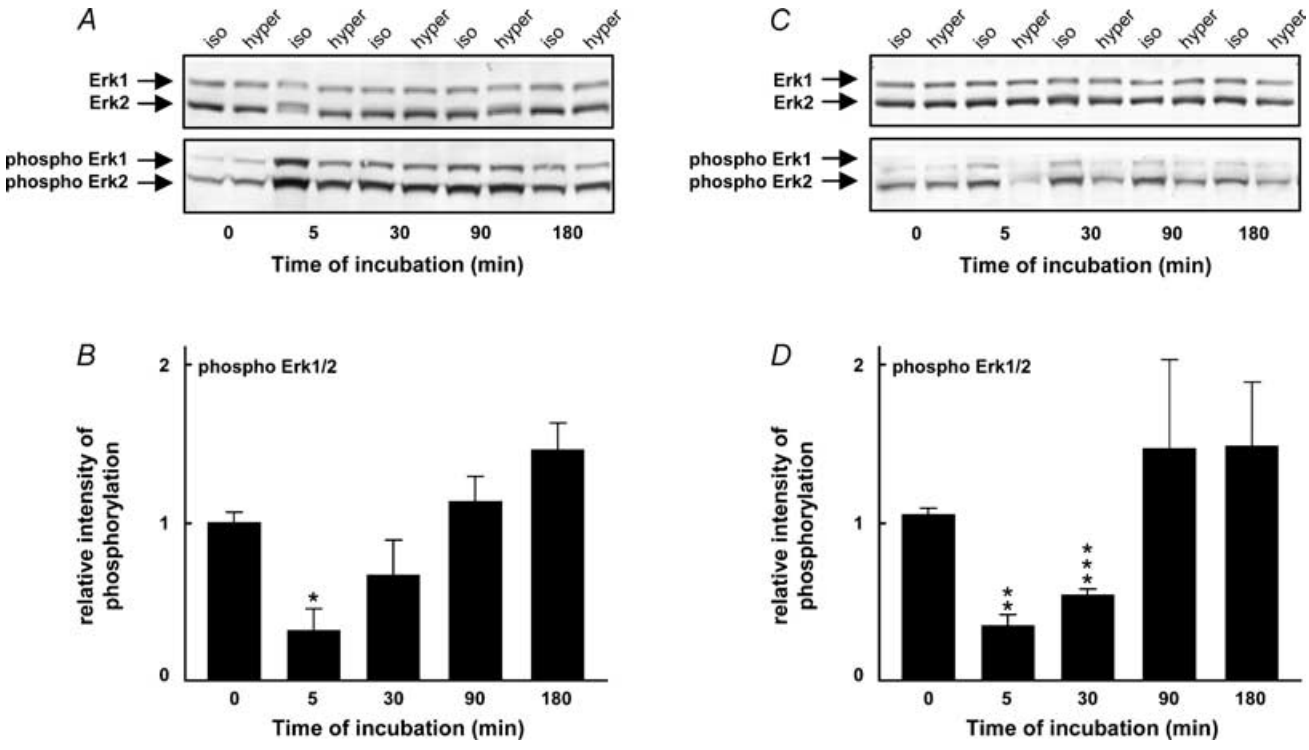

Figure 3. Level of Erk1/2 phosphorylation in hypertonic medium
A, NIH 3T3 cells were incubated in either isotonic (337 mosmol l^{-1}) or hypertonic (high NaCl) DMEM (687 mosmol l^{-1}), and cell lysates were subjected to SDS-PAGE and Western blot analysis at various time intervals. Specific antibodies against Erk1/2 (rabbit anti-Erk1/2) and phospho-Erk1/2 (rabbit antiphospho-Erk1/2) were used. *B*, intensity of Erk1/2 (p42) phosphorylation in hypertonic medium relative to the isotonic control. $^{*}P < 0.05$, $^{**}P < 0.01$, $^{***}P < 0.001$, significantly different from the isotonic control. The number of independent experiments was ≥ 5. *C* and *D*, NIH3T3 cells were incubated in isotonic (337 mosmol l^{-1}) DMEM and at time 0, concentrated NaCl or a similar amount of vehicle was added to the cells. The number of independent experiments was 3.

(687 mosmol l^{-1}) was studied using antibodies against non-phosphorylated and phosphorylated forms of p53 in Western blot and immunofluorescence microscopy analysis. From Fig. 5*A* and *B* it is seen that p53 is phosphorylated on serine in position 15 (S15) after about 30 min of high salt and that the phosphorylation increases up to at least 180 min. On the other hand we were unable to detect changes in the phosphorylation level of p53 on serines in positions 6, 9, 19, 37, 46 and 392 (Fig. 5*C*). To verify that phosphorylation of p53 on the serine in position 15 is a result of cell shrinkage and not of the increase in extracellular NaCl, the experiment was repeated with addition of sucrose to DMEM instead of NaCl to the same osmolarity. In two separate experiments the increase seen in p53 phosphorylation on S15 after addition of sucrose was identical to that seen after addition of high NaCl (Fig. 5*A* lower lane). Thus the p53 phosphorylation is a result of the cell shrinkage and not of the increased extracellular NaCl concentration as such.

As demonstrated in Fig. 5*D* phosphorylation of p53 in hypertonic medium is associated with a significant increase in the nuclear localization (blue) of p53 (red) and phospho-p53 (S15) (green). After 30 min in high salt medium we observed a strong increase in the level of phospho-p53 (S15) that was confined to the nucleus (green).

p38 acts upstream in relation to p53 and caspase-3 in the signalling pathway from shrinkage to apoptosis

p38 is well-known to act upstream in relation to the activation of p53 and caspase-3 (She *et al.* 2001; Kim *et al.* 2002; Zhu *et al.* 2002). To analyse whether this was the case during osmotic-induced apoptosis, osmotic shrinkage (687 mosmol l^{-1} for 4.5 h) was carried out on $RacV_{12}A_3$ cells preincubated with the p38 inhibitor SB203580 (10 μM) (Fig. 6). In these experiments

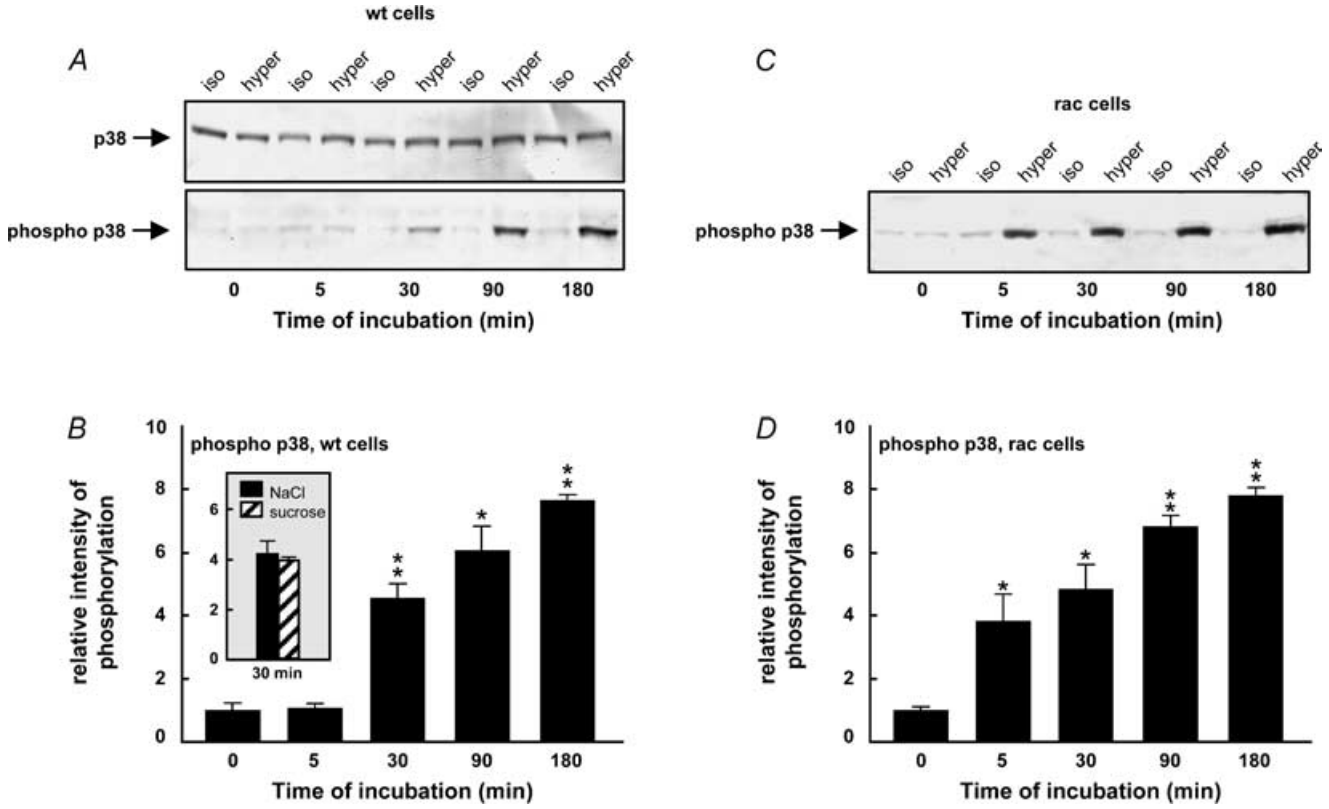

Figure 4. Level of p38 MAPK phosphorylation in hypertonic medium in wild-type NIH3T3 cells and in $RacV_{12}A_3$ cells

A, NIH 3T3 cells were incubated in either isotonic (337 mosmol l^{-1}) or hypertonic (high NaCl) medium (687 mosmol l^{-1}), and cell lysates were subjected to SDS-PAGE and Western blot analysis at various time intervals. Specific antibodies against p38 (rabbit anti-p38) and phospho-p38 (rabbit anti-phospho-p38) were used. *B*, intensity of p38 MAPK phosphorylation in hypertonic NaCl medium relative to the isotonic control. The inset compares intensity of p38 MAPK phosphorylation after 30 min in hypertonic (high NaCl) medium and hypertonic (sucrose) medium (687 mosmol l^{-1}). Experiments in *C* and *D* are identical to the experiments in *A* and *B* but using cells expressing constitutively active Rac. The number of independent experiments was ≥ 5. The error bars indicate standard error. $^*P < 0.05$, $^{**}P < 0.01$, significantly different from the isotonic control.

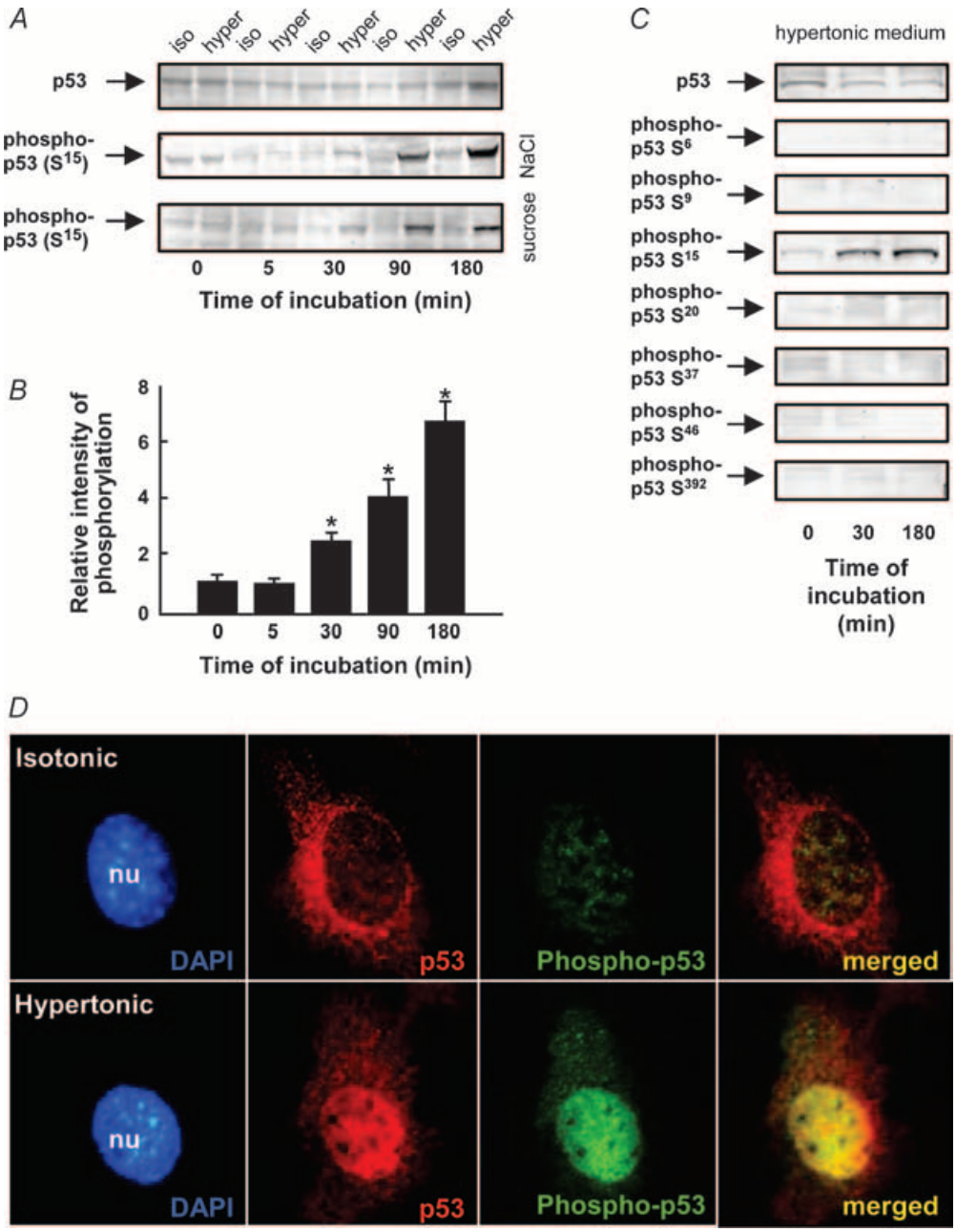

Figure 5. Level of p53 phosphorylation and subcellular localization of p53 and phospho-p53 in hypertonic medium

A, NIH 3T3 cells were incubated in either isotonic (337 mosmol l^{-1}), hypertonic (high NaCl) medium (687 mosmol l^{-1}) or hypertonic (sucrose) medium (687 mosmol l^{-1}), and cell lysates were subjected to SDS-PAGE and Western blot analysis at various time intervals. Specific antibodies against p53 (mouse anti-p53) and phospho-p53 (rabbit anti-phospho-p53 S15) were used. *B*, intensity of p53 phosphorylation in hypertonic (high NaCl) medium relative to the isotonic control. The error bars indicate standard error. $*P < 0.05$, significantly different from the isotonic control. The number of independent experiments was 5 except for the sucrose experiment where $n = 2$. *C*, SDS-PAGE and Western blot analysis of p53 phosphorylation at serine in positions 6, 9, 15, 20, 37, 46 and 392 after 0, 30 and 180 min of incubation of cells in high salt medium (687 mosmol l^{-1}). *D*, subcellular localization of p53 and phospho-p53. Immunolocalization of rabbit anti-p53 (red) and mouse anti-phospho-p53 S15 (green) in NIH 3T3 cells 30 min after incubation in either isotonic (337 mosmol l^{-1}) or hypertonic (687 mosmol l^{-1}) medium. Nuclei, stained with 4′,6-diamidino-2-phenylindole (DAPI), appear blue. Typical of 3 independent experiments.

activation of caspase-3 and p53 was evaluated by Western blot analysis using antibodies directed against cleaved, activated caspase-3 and phosphorylated p53 (S15), respectively. Obviously, the p38 inhibitor reduced the hypertonic-induced activation of both p53 ($P < 0.01$, $n = 3$) and caspase-3 ($P < 0.05$, $n = 3$) by at least threefold compared to the control cells. To exclude the possibility that SB203580 has a direct effect on the phosphorylation of p53 or the activation of caspase-3, $RacV_{12}A_3$ cells were grown in isotonic media containing SB203580. No significant difference was observed in the phosphorylation of p53 or in the caspases 3-activity in the isotonic cells treated with SB203580 compared to the isotonic control cells. These results favour the conclusion that p38 is positioned upstream in relation to both p53 and caspase-3 in the signal transduction pathway from cell shrinkage to apoptosis.

Delayed shrinkage-induced increase in the efflux of taurine and K^+. Importance of the monomeric protein Rac

Loss of organic osmolytes and KCl followed by cell shrinkage is a hallmark of the apoptotic process (Maeno *et al.* 2000). Since caspase-3 activity is induced as a consequence of NaCl-induced cell shrinkage, the question remains whether an increase in the permeability to cations and organic osmolytes is still a part of the apoptotic process under these conditions. To evaluate this question, the efflux of [^{3}H]taurine and $^{86}Rb^+$ was measured from NIH 3T3 cells preloaded with the isotope in isotonic DMEM medium and exposed to hypertonic DMEM medium (687 mosmol l^{-1}). $^{86}Rb^+$ is a tracer for potassium (Pedersen *et al.* 2002). Briefly, cells were preincubated with $^{86}Rb^+$ (Fig. 7*A*) or [^{3}H]taurine (Fig. 7*B*) for 2 h in

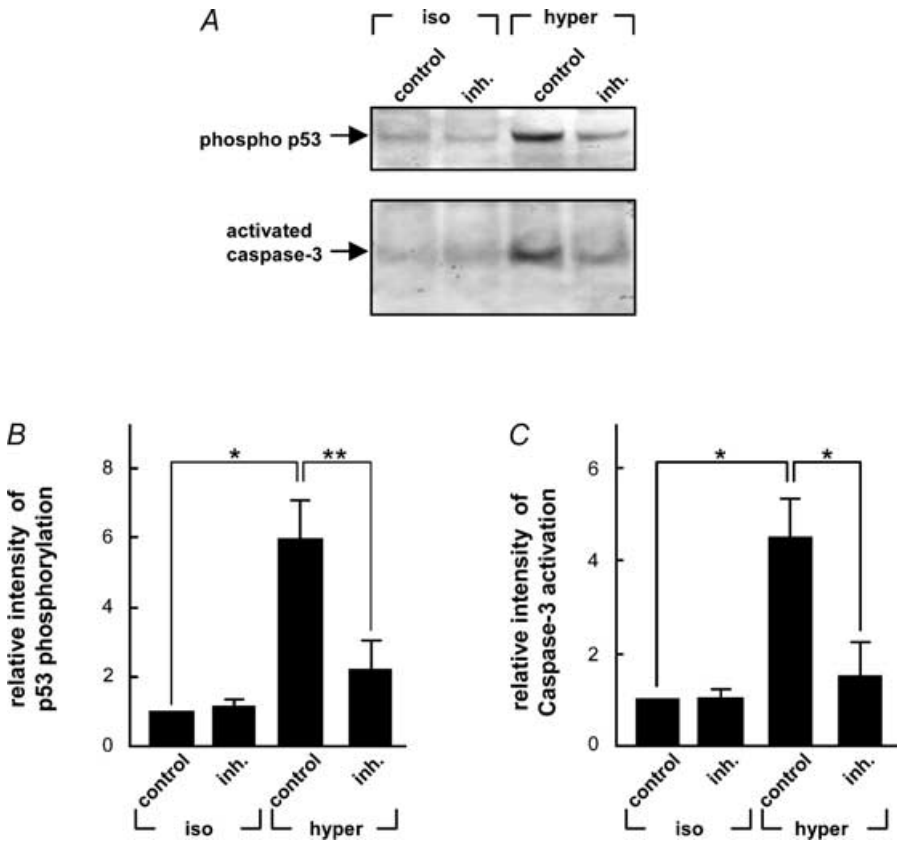

Figure 6. Level of p53 phosphorylation and caspase-3 activation in the presence of p38 inhibitor in hypertonic medium

A, $RacV_{12}A_3$ cells were preincubated for 1 h in isotonic (337 mosmol l^{-1}) medium and 10 μm SB203580 followed by 4.5 h incubation in hypertonic medium (687 mosmol l^{-1}). Cell lysates were prepared and subjected to SDS-PAGE and Western blot analysis. Specific antibodies against phospho-p53 (rabbit antiphospho-p53 S15) and cleaved caspase-3 (rabbit anticleaved caspase-3) were used. *B*, intensity of phospho-p53 S15 in isotonic medium containing SB203580 and hypertonic medium with and without SB203580 relative to isotonic control ($n = 3$). *C*, intensity of cleaved caspase-3 in isotonic medium containing SB203580 and hypertonic medium with and without SB203580 relative to the isotonic control ($n = 3$). $^*P < 0.05$, $^{**}P < 0.01$, significantly different from the isotonic control.

isotonic medium followed by incubation in hypertonic medium during which the rate constants for Rb^+ and taurine release were estimated over a 10-min period. The rate constant for $^{86}Rb^+$ efflux increased significantly ($P < 0.05$) at 90 min to $12.5 \times 10^{-3} \pm 2.79 \times 10^{-3}$ min^{-1}, $n = 8$) compared to the value obtained in isotonic medium ($5.2 \times 10^{-3} \pm 6.2 \times 10^{-4}$ min^{-1}, $n = 11$). The rate constant increased gradually to a maximum value of $37.6 \times 10^{-3} \pm 5.04 \times 10^{-3}$ min^{-1} ($P < 0.001$, $n = 8$) at 180 min. To see if the increase in the rate constant for $^{86}Rb^+$ is accompanied by an increase in the net permeability to K^+ we followed the K^+ content in a hypertonic NaCl medium with no K^+ as a function of time and observed a major loss of the cellular K^+ content after 90 min. However, the K^+ loss, which amounts to 0.096 ± 0.005 ($n = 3$) and 0.102 ± 0.001 μmol (mg protein)$^{-1}$ ($n = 3$) after 90 and 150 min, respectively, was compensated for by a quantitatively similar net uptake of Na^+ amounting to 0.11 ± 0.06 ($n = 3$) and 0.08 ± 0.03 μmol (mg protein)$^{-1}$ ($n = 3$), respectively, indicating that a non-selective channel rather that a specific K^+ channel has been activated around 90 min after cell shrinkage. The efflux of [^{3}H]taurine increased as a function of time following a pattern similar to that of $^{86}Rb^+$. From an isotonic level of $2.0 \times 10^{-3} \pm 1.7 \times 10^{-4}$ min^{-1} ($n = 11$), the rate constant increased significantly to $3.3 \times 10^{-3} \pm 4.1 \times 10^{-4}$ min^{-1} ($P < 0.01$, $n = 10$) after 60 min in hypertonic medium and further to a maximal rate constant of $24 \times 10^{-3} \pm 5.8 \times 10^{-3}$ min^{-1} ($P < 0.01$, $n = 8$) after 180 min. This is an 11.5-fold increase in the rate constant of taurine efflux. Thus in the period 60–90 min there is a dramatic increase in K^+, Na^+ and taurine permeabilities. To see whether the increased K^+ permeability is accompanied by a loss of cellular K^+ in the hypertonic DMEM at the time where caspase-3 is activated, we measured the K^+ content in cells exposed to either isotonic DMEM or to hypertonic medium for 4.5 h. We found no significant decrease in the cellular K^+ content, which was 0.21 ± 0.02 and 0.24 ± 0.05 μmol (mg protein)$^{-1}$ in isotonic and hypertonic medium, respectively (means ± S.E.M.; $n = 3$). The K^+ concentration in the DMEM is 5.8 mM and it is apparently enough to keep the balance between influx and efflux of K^+ even in the presence of a higher K^+ permeability.

Experiments carried out for wild-type cells were repeated using $RacV_{12}A_3$ cells (Fig. 7*A* and *B* rac cells). The rate constant for $^{86}Rb^+$ efflux increased to the same maximum value but the increase was larger at 60–120 min after incubation in hypertonic medium in $RacV_{12}A_3$ cells compared to that of wild-type cells (Fig. 7*A*). As an example, the rate constant for $RacV_{12}A_3$ cells after 90 min was about twofold higher ($24.9 \times 10^{-3} \pm 4.83 \times 10^{-3}$ min^{-1}) than that in wild-type cells ($12.5 \times 10^{-3} \pm 2.79 \times 10^{-3}$ min^{-1}). Figure 7*B* shows the results for taurine efflux in $RacV_{12}A_3$ cells compared to wild-type cells, which also showed a faster initiation in the increase in the rate constant of [^{3}H]taurine efflux in hypertonic medium compared to the wild-type cells. From an isotonic level of $1.84 \times 10^{-3} \pm 0.45 \times 10^{-3}$ ($n = 5$), the rate constant increased significantly to $6.3 \times 10^{-3} \pm 2.1 \times 10^{-3}$ ($P < 0.05$, $n = 5$) after 60 min in hypertonic medium and further to a maximal rate constant of $2.76 \times 10^{-2} \pm 0.82 \times 10^{-2}$ min^{-1} ($P < 0.05$, $n = 3$) after 180 min. The maximal rate constant measured for taurine efflux after 180 min in hypertonic solution was 15-fold higher than in isotonic control cells. Thus, Rac seems involved in the shrinkage-induced loss of osmolytes.

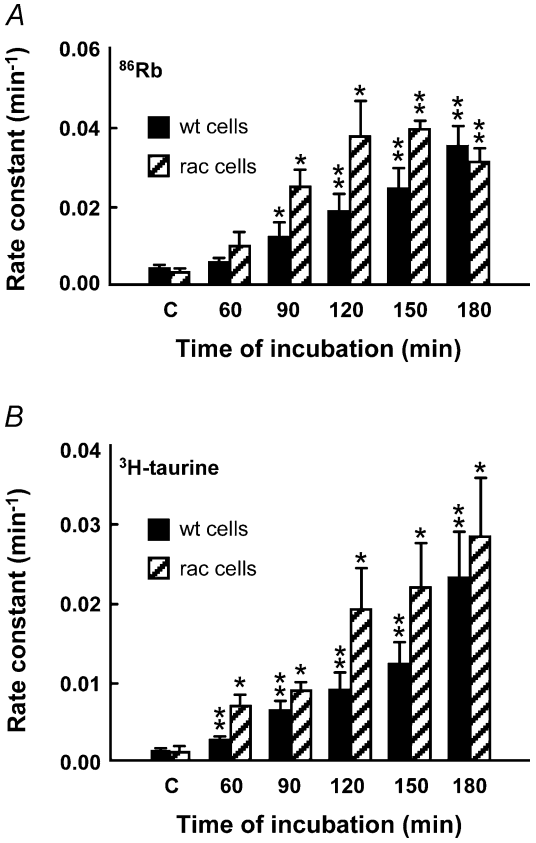

Figure 7. Effect of exposure to hypertonic NaCl on the rate constant for taurine and K^+ efflux in wild-type NIH 3T3 cells and in $RacV_{12}A_3$ cells

Cells grown at 80% confluence were loaded with [^{3}H]taurine and $^{86}Rb^+$ for 2 h and subsequently exposed to hypertonic DMEM (687 mosmol l^{-1}) in the time period indicated on the abscissa. [^{3}H]Taurine and $^{86}Rb^+$ release from the cells was followed at 2 min intervals in a 10-min period, and the rate constants (min^{-1}) for the $^{86}Rb^+$ loss (*A*) and for the [^{3}H]taurine loss (*B*) were estimated from the cellular fraction lost to the extracellular compartment during the efflux experiment. Values are given as means ± S.E.M. for $n = 3$ (*A*), $n = 3$ (*B*) and $n = 3$ (*C* and *D*) independent sets of experiments. $^*P < 0.05$, $^{**}P < 0.01$, significantly different from the isotonic control.

Discussion

Morphological changes and caspase-3 activity upon hypertonic cell shrinkage in NIH 3T3 cells

We have previously shown that if NIH 3T3 cells are re-exposed to isotonic medium after 15–20 min in hypotonic medium (the so called RVI after RVD protocol) they respond with rapid osmotic shrinkage and a fast subsequent RVI (∼55% volume recovery in 10 min) (Pedersen *et al.* 2002). As has been described for many other cell types (Hoffmann & Dunham, 1995) the fast RVI process in the RVD/RVI protocol is in contrast to the very slow RVI process seen after direct addition of high salt where the volume recovery after 0.5 and 1.5 h was only 29% and 40%, respectively (Fig. 1*A*). Actually, as seen from Fig. 1*B*, the cells never regained their original shape but remained in a contracted state with in an increasing number of apoptotic-like cytoplasmatic bodies surrounding the cells. Thus after 3 h in hypertonic medium the cells clearly seemed to enter into apoptosis. This was confirmed by measurements of the activity of caspase-3 in response to NaCl-induced cell shrinkage. A maximal and fivefold increase in caspase-3 activity was observed at 687 mosmol l^{-1} after 4.5 h and a moderate but significant increase was seen already after 1.5 h increasing significantly after 3 h. Thus, NaCl-induced cell shrinkage is clearly associated with an increase in the activity of caspase-3. Using propidium iodide staining we have also tested for necrosis (see Fig. 2*D*) and found no significant increase in the level of necrotic cells up to 4.5 h in 687 mosmol l^{-1} medium. High concentration of salt (650 mosmol l^{-1}) has previously been shown to cause apoptosis indicated by both changes in cellular morphology and caspase-3 activation in renal inner medullary epithelial cells (Michea *et al.* 2000; Burg, 2002; Zhang *et al.* 2002), and a high concentration of salt is found to result in activation of caspase-3 in several other cell types such as lymphocytes (Bortner *et al.* 1997), HeLa cells, PC12 cells (Okada *et al.* 2001) and rat hepatocytes (Reinehr *et al.* 2002). Whether hypertonicity-induced caspase-3 activity is adequate to initiate apoptosis *per se* apparently depends on the cell type used for investigation. Reinehr *et al.* (2002) showed that activation of caspase-3 by hyperosmotic exposure in hepatocytes essentially results in a sensitization towards CD95L-induced apoptosis. In lymphocytes and nerve cells, however, high salt above 500 mosmol l^{-1} leads to inter-nucleosomal DNA fragmentation, which is distinctive for the late events in apoptosis (Bortner *et al.* 1997; van Golen *et al.* 2000). Similarly, we here demonstrate that hypertonic exposure to NIH 3T3 cells may act through caspase-3 to initiate the apoptotic cascade, which includes the formation of apoptotic bodies. It should be noted that the increase in caspase-3 activity seen in the present investigation in NIH 3T3 cells after 4.5 h of hypertonic incubation is about 80% higher than that observed by Reinehr and coworkers in hepatocytes after 9 h of incubation in hypertonic medium. Thus the question whether cell shrinkage induces apoptosis as such or merely sensitizes the cells for this death mode needs further investigation.

Activation of MAP Kinases upon hypertonic cell shrinkage in NIH 3T3 cells

Generally, p38 MAP kinase activity is a signal for programmed cell death (Harper & LoGrasso, 2001; Zhu *et al.* 2002; Naderi *et al.* 2003). As p38 was found to be activated after cell shrinkage in several cell types (Schafer *et al.* 1998; Roger *et al.* 1999; Bode *et al.* 1999; Duzgun *et al.* 2000; Gillis *et al.* 2001; Pederson *et al.* 2002; Shen *et al.* 2002; Umenishi & Schrier, 2003; Bildin *et al.* 2003), we looked for p38 as an intermediate signal component that precedes increased osmolyte efflux and caspases-3 activity upon hypertonic stress in NIH 3T3 cells. We found that the level of p38 phosphorylation in NIH 3T3 cells was significantly increased after 30 min in hypertonic medium compared to the isotonic control (Fig. 4) and this level was further increased to about six- and eightfold at 90 and 180 min, respectively. These results show that p38 is activated prior to loss of K^+ and taurine as well as to activation of caspase-3 in NaCl-treated cells, and we suggest that p38 may act upstream in relation to these cellular events. A p38- and shrinkage-dependent activation of non-selective cation channels was previously demonstrated in human cervical cancer cells (Shen *et al.* 2002).

In contrast to p38, the phosphorylation level of Erk1/2 was considerably lower after 5 min in hypertonic medium compared to that of the isotonic control. This was followed by a gradual re-phosphorylation of Erk1/2 in the hypertonic treated cells during the following 3 h (Fig. 3), i.e. in the period where the cells regain their volume. It was previously shown that inhibition of Erk1/2 enhances deoxycholic acid-induced apoptosis in hepatocytes (Qiao *et al.* 2001). Thus the initial inhibition of Erk1/2 presented in the current report after addition of high salt could contribute to the apoptotic response of NIH 3T3 cells. For comparison, it has been shown that the choice between survival and apoptosis is controlled by the balance between the activity of p38 and Erk1/2 in PC12 cells (Xia *et al.* 1995). Further, phosphorylated p38 may physically interact with Erk1/2 and inhibit Erk1/2 phosphotransferase activity (Zhang *et al.* 2001). It is therefore likely that shrinkage-dependent activation of p38 and subsequent inhibition of Erk1/2 is important for the apoptotic effect of hypertonic stress in NIH 3T3 cells. In a human embryonic kidney cell line (293 cells), it was found that shrinkage-induced activation of p38 proceeded via the

monomeric G proteins Rac and CDC42 (Wesselborg *et al.* 1997), and possibly also via the p21 activated kinase (PAK) (Roig *et al.* 2000). These observations support our suggestion that Rac and p38 act in concert and upstream to the loss of K^+ and taurine as well as to the activation of caspase-3 during hypertonic stress in NIH 3T3 cells.

The role of osmolytes during apoptosis and hypertonic cell shrinkage in NIH 3T3 cells

Loss of organic osmolytes and KCl has been suggested to be an essential part of the apoptotic process. There is evidence in the literature that a decrease in K^+ concentration is necessary for activation of caspases to occur (Dallaporta *et al.* 1998; Hughes & Cidlowski, 1999; Platoshyn *et al.* 2002), and in lymphocytes Lang and coworkers demonstrated a late increase in taurine permeability after induction of CD95-induced apoptosis (Lang *et al.* 1998*c*; Lang *et al.* 2000*a*). Since, in the present report, caspase-3 activity is induced as a consequence of NaCl-induced cell shrinkage, which will result in an increase in the cellular concentration of organic osmolytes and KCl, the question remains whether an eventual later increase in the permeability to cations and organic osmolytes should occur. To evaluate this question the efflux of [^{3}H]taurine and $^{86}Rb^+$ was measured from cells treated with hypertonic medium (687 mosmol l^{-1}). As seen from Fig. 7 the rate constant for taurine and $^{86}Rb^+$ efflux increased significantly at 60 and 90 min, respectively, and reached a maximal value at 180 min. Such a late increase in taurine permeability is very similar to what has been described in lymphocytes (Lang *et al.* 2000*a*); the importance for the apoptotic process in the fibroblasts has not yet been studied. The increase in the rate constant for $^{86}Rb^+$ is accompanied by an increase in the net permeability to K^+ concomitant with an increase in the net permeability to Na^+. Since the increase in net K^+ permeability took place concomitant with a similar increase in the net Na^+ permeability it is likely that a shrinkage-induced non-selective cation channel is responsible. Such channels have been described in several cell types (Koch & Korbmacher, 2000; Kellenberger & Schild, 2002; Lawonn *et al.* 2003; Wehner *et al.* 2003). The increase in net K^+ permeability did not, however, result in any significant decrease in the cellular K^+ content after 4.5 h in the hypertonic DMEM. The 5.8 mM K^+ in the DMEM is apparently enough to keep the balance between influx of K^+ via the Na^+,K^+,$2Cl^-$ cotransporter and the Na^+,K^+-ATPase and efflux of K^+ via leak pathways even in the presence of an increased K^+ permeability. Thus, no loss of cellular K^+ precedes the activation of caspase-3 by high salt. This is important since K^+ is known to be a negative regulator of caspases (Hughes. & Cidlowski, 1999; Platoshyn *et al.* 2002). The effect of cell shrinkage in the present investigation thus clearly results from the shrinkage *per se* and not from a secondary loss of K^+.

Rac is upstream shrinkage activation of p38, caspase-3 and K^+ and taurine permeabilities

It was previously found that the RVI process in the RVD/RVI protocol is more efficient in $RacV_{12}A_3$ cells (~100% volume recovery in 20 min) compared to wild-type cells (~65% volume recovery in 20 min) pointing to the small G-protein Rac as a candidate in the signalling cascade from cell shrinkage to RVI (Beisner, 2004). In the present paper we present evidence that Rac is also a candidate in the signalling cascade between cell shrinkage and caspase-3 based on the following observations: (i) the activity of caspase-3 induced by hypertonicity is higher in $RacV_{12}A_3$ cells compared to wild-type cells, i.e. the caspase-3 activity at 4.5 h was threefold higher compared to that obtained with wild-type cells; (ii) p38 was phosphorylated at an increased rate in $RacV_{12}A_3$ cells; and (iii) the rate constant for K^+ efflux in NIH 3T3 $RacV_{12}A_3$ cells initiated earlier and more dramatically after incubation in hypertonic medium compared to that of wild-type cells. Taurine efflux in $RacV_{12}A_3$ cells also showed a faster initiation in the increase in the rate constant in hypertonic medium compared to the wild-type cells. The maximal rate constant measured for taurine efflux after 180 min in hypertonic solution was 15-fold higher than in isotonic control cells. Thus, Rac is important for the shrinkage-induced p38 and caspase-3 activation as well as for the increase in cellular permeability to cations and organic osmolytes. It has been suggested that the protein complex of Rac-Osm-MEKK3-MKK3 that activates p38 in response to hypertonicity in mammalian cells is the mammalian counterpart of the osmosensing CDC42-STE50-Ste11-PBS2-Hog1 signal pathway of *S. cerevisiae* (Uhlik *et al.* 2003). Our results are in agreement with this proposal.

Activation of p53 upon hypertonic cell shrinkage in NIH 3T3 cells

The multifunctional transcription factor p53 is a tumour suppressor that has various defects in many cancer cells (Bargonetti & Manfredi, 2002). The activity of p53 is regulated by serine/threonine phosphorylation and by lysine acetylation (Hupp *et al.* 2000). p38, which was found to be activated after cell shrinkage in NIH 3T3 fibroblasts in the present investigation, is known to activate p53 (Sanchez-Prieto *et al.* 2000; She *et al.* 2001; Kim *et al.* 2002; Zhu *et al.* 2002). Upon phosphorylation, p53 translocates to the nucleus and signals arrest of cell growth or alternatively serves as an activator of apoptosis depending on the degree and the time course of cellular damage (see,

e.g. Haupt *et al.* 2003). In this report we show that elevation of the osmolarity to 687 mosmol l^{-1} by addition of NaCl, significantly phosphorylates p53 on S15 after about 30 min (Fig. 5*A* and *B*) and this phosphorylation is associated with a significant increase in the nuclear localization of both p53 and phospho-p53 (S15) (Fig. 5*D*). The phosphorylation level was further increased to about four- and sevenfold at 90 and 180 min, respectively (Fig. 5*B*). Phosphorylation of p53 on S15 is known to inhibit p53-MDM2 (mouse double minute 2) interactions giving higher stability to p53 and increasing the affinity for the coactivator, p300/CPB, which leads to lysine acetylation of p53 (Dumaz & Meek, 1999; Stewart & Pietenpol, 2001). In the present investigation, increased activity of p53 by S15 phosphorylation clearly precedes the increase in caspase-3 activation and the increase in permeability to cations and taurine, supporting the conclusion that p53, as for p38, is activated upstream in relation to these events. In renal inner medullary cells, it was found that phosphorylation of p53 on S15 peaks at 600 mosmol l^{-1} and then decreases substantially at 700 and 800 mosmol l^{-1}. Preliminary results from our group on NIH 3T3 cells show that the NaCl concentration dependence of increased abundance of the S15 phosphorylation varies slightly from renal medullary cells in that it seems to be maximal around 637–687 mosmol l^{-1}. In medullary cells, the increase in p53 phosphorylation at 500 mosmol l^{-1} is protective against apoptosis whereas 700 mosmol l^{-1} induces apoptosis. We observe very little caspase-3 activation at 637 mosmol l^{-1} (see Fig. 2*A*) although the level of p53 phosphorylation is higher than that seen at 687 mosmol l^{-1} (K. Schou, S. T. Christensen and E. K. Hoffmann, unpublished observations). Thus, it is possible that p53 also has a protective effect in NIH 3T3 cells at lower osmolarities whereas p53 at higher osmolarities like 687 mosmol l^{-1} supports the apoptotic cascade through activation of caspase-3. This question is under further investigation. There are many examples that p53-mediated apoptosis proceeds through the effector caspases like caspase-3 (see Schuler & Green, 2001). p53 up-regulates the expression of death receptors Fas and DR5 (Sheikh & Fornace, 2000) and the pro-apoptotic Bcl-2 family proteins such as Bax, which induces mitochondrial cytochrome *c* release (Schuler *et al.* 2003; Mihara *et al.* 2003; Schuler & Green, 2005). Moreover, p53 is reported to physically interact with antiapoptotic proteins in the mitochondria (Sheikh & Fornace, 2000; Chipuk *et al.* 2004).

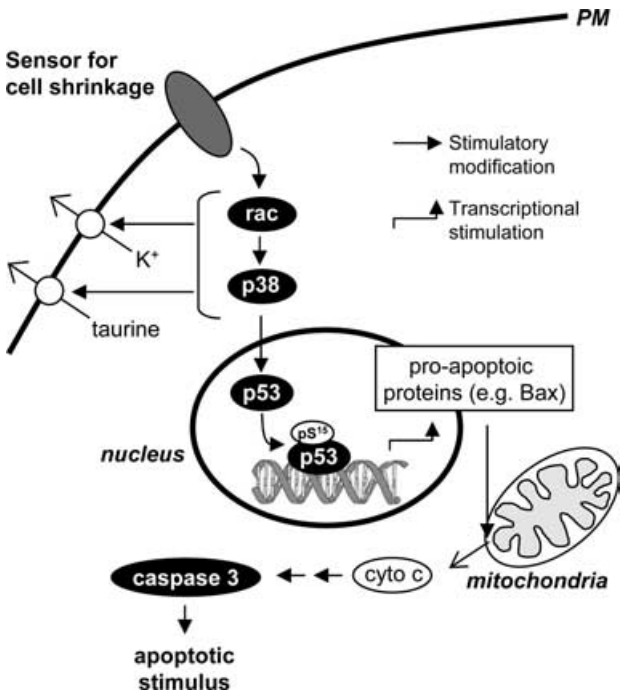

Figure 8. Proposed sequence of signal events in the cell shrinkage-induced Caspase3 activation
Cellular shrinkage detected by an unknown volume sensor activates Rac and p38, followed by permeability increases to K^+ and taurine and phosphorylation and nuclear translocation of p53, resulting in caspase-3 activation. Black boxes indicate experimental evidence; white boxes indicate the action of possible, transitional signal events.

p38 is upstream shrinkage activation of p53 and caspase-3

We find that inhibition of p38 reduces hypertonic-induced activation of caspase-3 and p53, demonstrating that p38 is required for full activation of both caspase-3 and p53 and that p38 is positioned upstream from caspase-3 and p53 in the signal transduction pathway from shrinkage to apoptosis. Indeed, p38 is a known mediator of osmostress responses (Sheikh-Hamad & Gustin, 2004) and an activator of p53 in several cell types undergoing apoptosis (Sanchez-Prieto *et al.* 2000; She *et al.* 2001; Kishi *et al.* 2001; Kim *et al.* 2002; Zhu *et al.* 2002).

In conclusion, our results indicate that the following sequence of signalling events is involved in shrinkage-induced apoptosis in NIH 3T3 cells (see Fig. 8). Hypertonic shrinkage activates the small G protein Rac, which via PAK then activates the MAP kinase p38. p38 then inhibits Erk1/2 and activates p53 and non-selective cation channels as well as organic osmolyte channels. Caspase-3 is subsequently activated by a p38-dependent pathway, which may involve the following steps: phosphorylated p53 is translocated to the nucleus where, among other regulatory events, it stimulates the transcription of pro-apoptotic molecules, e.g. Bax, resulting in Cyt *c* release, caspase-9 stimulation and finally stimulation of caspase-3. Alternative p53-independent pathways from p38 to caspase-3 activation are under investigation.

References

Anbari K & Schultz RM (1993). Effect of sodium and betaine in culture media on development and relative rates of protein synthesis in preimplantation mouse embryos in vitro. *Mol Reprod Dev* **35**, 24–28.

Aznar S, Fernandez-Valeron P, Espina C & Lacal JC (2004). Rho GTPases: potential candidates for anticancer therapy. *Cancer Lett* **206**, 181–191.

Bargonetti J & Manfredi JJ (2002). Multiple roles of the tumor suppressor p53. *Current Opinion Oncol* **14**, 86–91.

Beisner KH (2004). Volume regulation in NIH-3T3 fibroblasts: Effect of constitutively active RhoA, Rac1 and H-Ras. Masters Thesis. August Krogh Institute, University of Copenhagen.

Best L, Sheader EA & Brown PD (1996). A volume-activated anion conductance in insulin-secreting cells. *Pflugers Arch* **431**, 363–370.

Bildin VN, Wang Z, Iserovich P & Reinach PS (2003). Hypertonicity-induced p38MAPK activation elicits recovery of corneal epithelial cell volume and layer integrity. *J Membrane Biol* **193**, 1–13.

Bode JG, Gatsios P, Ludwig S, Rapp UR, Haussinger D, Heinrich PC & Graeve L (1999). The mitogen-activated protein (MAP) kinase p38 and its upstream activator MAP kinase kinase 6 are involved in the activation of signal transducer and activator of transcription by hyperosmolarity. *J Biol Chem* **274**, 30222–30227.

Bortner CD & Cidlowski JA (1996). Absence of volume regulatory mechanisms contributes to the rapid activation of apoptosis in thymocytes. *Am J Physiol* **271**, C950–C961.

Bortner CD & Cidlowski JA (1998). A necessary role for cell shrinkage in apoptosis. *Biochem Pharmacol* **56**, 1549–1559.

Bortner CD & Cidlowski JA (2003). Uncoupling cell shrinkage from apoptosis reveals that Na^+ influx is required for volume loss during programmed cell death. *J Biol Chem* **278**, 39176–39184.

Bortner CD & Cidlowski JA (2004). The role of apoptotic volume decrease and ionic homeostasis in the activation and repression of apoptosis. *Pflugers Arch* **448**, 313–318.

Bortner CD, Hughes FM Jr & Cidlowski JA (1997). A primary role for K^+ and Na^+ efflux in the activation of apoptosis. *J Biol Chem* **272**, 32436–32442.

Burg MB (2002). Response of renal inner medullary epithelial cells to osmotic stress. *Comp Biochem Physiol A Mol Integr Physiol* **133**, 661–666.

Chipuk JE, Kuwana T, Bouchier-Hayes L, Droin NM, Newmeyer DD, Schuler M & Green DR (2004). Direct activation of Bax by p53 mediates mitochondrial membrane permeabilization and apoptosis. *Science* **303**, 1010–1014.

Dallaporta B, Hirsch T, Susin SA, Zamzami N, Larochette N, Brenner C, Marzo I & Kroemer G (1998). Potassium leakage during the apoptotic degradation phase. *J Immunol* **160**, 5605–5615.

De Nadal E, Alepuz PM & Posas F (2002). Dealing with osmostress through MAP kinase activation. *EMBO Rep* **3**, 735–740.

Dmitrieva N, Kultz D, Michea L, Ferraris J & Burg M (2000). Protection of renal inner medullary epithelial cells from apoptosis by hypertonic stress-induced p53 activation. *J Biol Chem* **275**, 18243–18247.

Dmitrieva N, Michea L & Burg M (2001*a*). p53 protects renal inner medullary cells from hypertonic stress by restricting DNA replication. *Am J Physiol Renal Physiol* **281**, F522–F530.

Dmitrieva NI, Michea LF, Rocha GM & Burg MB (2001*b*). Cell cycle delay and apoptosis in response to osmotic stress. *Comp Biochem Physiol A Mol Integr Physiol* **130**, 411–420.

Dumaz N & Meek DW (1999). Serine15 phosphorylation stimulates p53 transactivation but does not directly influence interaction with HDM2. *EMBO J* **18**, 7002–7010.

Duzgun SA, Rasque H, Kito H, Azuma N, Li W, Basson MD, Gahtan V, Dudrick SJ & Sumpio BE (2000). Mitogen-activated protein phosphorylation in endothelial cells exposed to hyperosmolar conditions. *J Cell Biochem* **76**, 567–571.

Gillis D, Shrode LD, Krump E, Howard CM, Rubie EA, Tibbles LA, Woodgett J & Grinstein S (2001). Osmotic stimulation of the Na^+/H^+ exchanger NHE1: relationship to the activation of three MAPK pathways. *J Membr Biol* **181**, 205–214.

Harper SJ & LoGrasso P (2001). Signalling for survival and death in neurones. the role of stress-activated kinases, JNK and p38. *Cell Signal* **13**, 299–310.

Haupt S, Berger M, Goldberg Z & Haupt Y (2003). Apotosis – the p53 network. *Cell Science* **116**, 4077–4085.

Hoffmann EK & Dunham PB (1995). Membrane mechanisms and intracellular signalling in cell volume regulation. *Int Rev Cytol* **161**, 173–262.

Hoffmann EK, Jessen F & Dunham PB (1994). The Na-K-2Cl cotransporter is in a permanently activated state in cytoplasts from Ehrlich ascites tumor cells. *J Membr Biol* **138**, 229–239.

Hoffmann EK & Pedersen SF (1998). Sensors and signal transduction in the activation of cell volume regulatory ion transport systems. *Contrib Nephrol* **123**, 50–78.

Hoffmann EK & Simonsen LO (1989). Membrane mechanisms in volume and pH regulation in vertebrate cells. *Physiol Rev* **69**, 315–382.

Hughes FM Jr & Cidlowski JA (1999). Potassium is a critical regulator of apoptotic enzymes in vitro and in vivo. *Adv Enzyme Regul* **39**, 157–171.

Hupp TR, Lane DP & Ball KL (2000). Strategies for manipulating the p53 pathway in the treatment of human cancer. *Biochem J* **352**, 1–17.

Kellenberger S & Schild L (2002). Epithelial sodium channel/degenerin family of ion channels: a variety of functions for a shared structure. *Physiol Rev* **82**, 735–767.

Kim SJ, Hwang SG, Shin DY, Kang SS & Chun JS (2002). p38 kinase regulates nitric oxide-induced apoptosis of articular chondrocytes by accumulating p53 via NFkappa B-dependent transcription and stabilization by serine 15 phosphorylation. *J Biol Chem* **277**, 33501–33508.

Kishi H, Nakagawa K, Matsumoto M, Suga M, Ando M, Taya Y & Yamaizumi M (2001). Osmotic shock induces G1 arrest through p53 phosphorylation at Ser33 by activated p38MAPK without phosphorylation at Ser15 and Ser20. *J Biol Chem* **276**, 39115–39122.

Koch JP & Korbmacher C (2000). Mechanism of shrinkage activation of nonselective cation channels in M-1 mouse cortical collecting duct cells. *J Membr Biol* **177**, 231–242.

Krick S, Platoshyn O, Sweeney M, Kim H & Yuan JX (2001). Activation of K^+ channels induces apoptosis in vascular smooth muscle cells. *Am J Physiol Cell Physiol* **280**, C970–C979.

Lang F, Busch GL, Ritter M, Völkl H, Waldegger S, Gulbins E & Häussinger D (1998*a*). Functional significance of cell volume regulatory mechanisms. *Physiol Rev* **78**, 247–306.

Lang KS, Fillon S, Schneider D, Rammensee HG & Lang F (2002). Stimulation of TNF alpha expression by hyperosmotic stress. *Pflugers Arch* **443**, 798–803.

Lang F, Lang KS, Wieder T, Myssina S, Birka C, Lang PA, Kaiser S, Kempe D, Duranton C & Huber SM (2003). Cation channels, cell volume and the death of an erythrocyte. *Pflugers Arch* **447**, 121–125.

Lang F, Lepple-Wienhues A, Szabó I, Siemen D & Gulbins E (1998*b*). Cell volume in cell proliferation and apoptotic cell death. In *Cell Volume Regulation*, ed. Lang F, pp. 158–168. Karger, Basel.

Lang F, Madlung J, Siemen D, Ellory C, Lepple-Wienhues A & Gulbins E (2000*a*). The involvement of caspases in the CD95 (Fas/Apo-1) -but not swelling-induced cellular taurine release from Jurkat T-lymphocytes. *Pflugers Arch* **440**, 93–99.

Lang F, Madlung J, Uhlemann AC, Risler T & Gulbins E (1998*c*). Cellular taurine release triggered by stimulation of the Fas (CD95) receptor in Jurkat lymphocytes. *Pflugers Arch* **436**, 377–383.

Lang F, Ritter M, Gamper N, Huber S, Fillon S, Tanneur V, Lepple-Wienhues A, Szabo I & Gulbins E (2000*b*). Cell volume in the regulation of cell proliferation and apoptotic cell death. *Cell Physiol Biochem* **10**, 417–428.

Lawonn P, Hoffmann EK, Hougaard C & Wehner F (2003). A cell shrinkage-induced non-selective cation conductance with a novel pharmacology in Ehrlich-Lettre-ascites tumour cells. *FEBS Lett* **539**, 115–119.

Maeno E, Ishizaki Y, Kanaseki T, Hazama A & Okada Y (2000). Normotonic cell shrinkage because of disordered volume regulation is an early prerequisite to apoptosis. *Proc Natl Acad Sci U S A* **97**, 9487–9492.

Michea L, Ferguson DR, Peters EM, Andrews PM, Kirby MR & Burg MB (2000). Cell cycle delay and apoptosis are induced by high salt and urea in renal medullary cells. *Am J Physiol Renal Physiol* **278**, F209–F218.

Mihara M, Erster S, Zaika A, Petrenko O, Chittenden T, Pancoska P & Moll UM (2003). p53 has a direct apoptogenic role at the mitochondria. *Mol Cell* **11**, 577–590.

Moran J, Hernandez-Pech X, Merchant-Larios H & Pasantes-Morales H (2000). Release of taurine in apoptotic cerebellar granule neurons in culture. *Pflugers Arch* **439**, 271–277.

Naderi J, Hung M & Pandey S (2003). Oxidative stress-induced apoptosis in dividing fibroblasts involves activation of D38 MAP kinase and over-expression of Bax: Resistance of quiescent cells to oxidative stress. *Apoptosis* **8**, 91–100.

Nilius B (2001). Chloride channels go cell cycling. *J Physiol* **532**, 581.

Okada Y, Maeno E, Shimizu T, Dezaki K, Wang J & Morishima S (2001). Receptor-mediated control of regulatory volume decrease (RVD) and apoptotic volume decrease (AVD). *J Physiol* **532**, 3–16.

Pedersen SF, Beisner KH, Hougaard C, Willumsen BM, Lambert IH & Hoffmann EK (2002). Rho family GTP binding proteins are involved in the regulatory volume decrease process in NIH3T3 mouse fibroblasts. *J Physiol* **541**, 779–796.

Pederson SF, Varming C, Christensen ST & Hoffmann EK (2002). Mechanisms of activation of NHE by cell shrinkage and by calyculin A in Ehrlich ascites tumor cells. *J Membr Biol* **189**, 67–81.

Platoshyn O, Zhang S, McDaniel SS & Yuan JXJ (2002). Cytochrome c activates K^+ channels before inducing apoptosis. *Am J Physiol Cell Physiol* **283**, C1298–C1305.

Qiao L, Studer E, Leach K, McKinstry R, Gupta S, Decker R, Kukreja R, Valerie K, Nagarkatti P, El Deiry W, Molkentin J, Schmidt-Ullrich R, Fisher PB, Grant S, Hylemon PB & Dent P (2001). Deoxycholic acid (DCA) causes ligand-independent activation of epidermal growth factor receptor (EGFR) and FAS receptor in primary hepatocytes: inhibition of EGFR/mitogen-activated protein kinase-signaling module enhances DCA-induced apoptosis. *Mol Biol Cell* **12**, 2629–2645.

Qin S, Ding J, Takano T & Yamamura H (1999). Involvement of receptor aggregation and reactive oxygen species in osmotic stress-induced Syk activation in B cells. *Biochem Biophys Res Commun* **262**, 231–236.

Reinehr R, Graf D, Fischer R, Schliess F & Haussinger D (2002). Hyperosmolarity triggers CD95-membrane trafficking and sensitizes rat hepatocytes towards CD95L-induced apoptosis. *Hepatology* **36**, 430A.

Roger F, Martin PY, Rousselot M, Favre H & Feraille E (1999). Cell shrinkage triggers the activation of mitogen-activated protein kinases by hypertonicity in the rat kidney medullary thick ascending limb of the Henle's loop. Requirement of p38 kinase for the regulatory volume increase response. *J Biol Chem* **274**, 34103–34110.

Roig J, Huang Z, Lytle C & Traugh JA (2000). p21-activated protein kinase gamma-PAK is translocated and activated in response to hyperosmolarity. Implication of Cdc42 and phosphoinositide 3-kinase in a two-step mechanism for gamma-PAK activation. *J Biol Chem* **275**, 16933–16940.

Sanchez-Prieto R, Rojas JM, Taya Y & Gutkind JS (2000). A role for the p38 mitogen-activated protein kinase pathway in the transcriptional activation of p53 on genotoxic stress by chemotherapeutic agents. *Cancer Res* **60**, 2464–2472.

Schafer C, Ross SE, Bragado MJ, Groblewski GE, Ernst SA & Williams JA (1998). A role for the p38 mitogen-activated protein kinase/Hsp 27 pathway in cholecystokinin-induced changes in the actin cytoskeleton in rat pancreatic acini. *J Biol Chem* **273**, 24173–24180.

Schuler M & Green DR (2001). Mechanisms of p53-dependent apoptosis. *Biochem Soc Trans* **29**, 684–688.

Schuler M & Green DR (2005). Transcription, apoptosis and p53: catch-22. *Trends Genet* **21**, 182–187.

Schuler M, Maurer U, Goldstein JC, Breitenbucher F, Hoffarth S, Waterhouse NJ & Green DR (2003). p53 triggers apoptosis in oncogene-expressing fibroblasts by the induction of Noxa and mitochondrial Bax translocation. *Cell Death Differentiation* **10**, 451–460.

She QB, Bode AM, Ma WY, Chen NY & Dong Z (2001). Resveratrol-induced activation of p53 and apoptosis is mediated by extracellular-signal-regulated protein kinases and p38 kinase. *Cancer Res* **61**, 1604–1610.

Sheikh MS & Fornace AJ (2000). Role of p53 family members in apoptosis. *J Cellular Physiol* **182**, 171–181.

Sheikh-Hamad D & Gustin MC (2004). MAP kinases and the adaptive response to hypertonicity: functional preservation from yeast to mammals. *Am J Physiol Renal Physiol* **287**, F1102–F1110.

Shen MR, Chou CY, Hsu KF & Ellory JC (2002). Osmotic shrinkage of human cervical cancer cells induces an extracellular Cl^--dependent nonselective cation channel, which requires p38 MAPK. *J Biol Chem* **277**, 45776–45784.

Stewart ZA & Pietenpol JA (2001). p53 Signaling and cell cycle checkpoints. *Chem Res Toxicol* **14**, 243–263.

Terada Y, Inoshita S, Hanada S, Shimamura H, Kuwahara M, Ogawa W, Kasuga M, Sasaki S & Marumo F (2001). Hyperosmolality activates Akt and regulates apoptosis in renal tubular cells. *Kidney Int* **60**, 553–567.

Uhlik MT, Abell AN, Johnson NL, Sun WY, Cuevas BD, Lobel-Rice KE, Horne EA, Dell'Acqua ML & Johnson GL (2003). Rac-MEKK3-MKK3 scaffolding for p38 MAPK activation during hyperosmotic shock. *Nature Cell Biol* **5**, 1104–1110.

Umenishi F & Schrier RW (2003). Hypertonicity-induced aquaporin-1 (AQP1) expression is mediated by the activation of MAPK pathways and hypertonicity-responsive element in the AQP1 gene. *J Biol Chem* **278**, 15765–15770.

van Golen CM, Castle VP & Feldman EL (2000). IGF-I. receptor activation and BCL-2 overexpression prevent early apoptotic events in human neuroblastoma. *Cell Death Differentiation* **7**, 654–665.

Wehner F, Shimizu T, Sabirov R & Okada Y (2003). Hypertonic activation of a non-selective cation conductance in HeLa cells and its contribution to cell volume regulation. *FEBS Lett* **551**, 20–24.

Wesselborg S, Bauer MKA, Vogt M, Schmitz ML & Schulze-Osthoff K (1997). Activation of transcription factor NF-kappaB and p38 mitogen-activated protein kinase is mediated by distinct and separate stress effector pathways. *J Biol Chem* **272**, 12422–12429.

Xia Z, Dickens M, Raingeaud J, Davis RJ & Greenberg ME (1995). Opposing effects of ERK and JNK-p38 MAP kinases on apoptosis. *Science* **270**, 1326–1331.

Zhang Z, Cai Q, Michea L, Dmitrieva NI, Andrews P & Burg MB (2002). Proliferation and osmotic tolerance of renal inner medullary epithelial cells in vivo and in cell culture. *Am J Physiol Renal Physiol* **283**, F302–F308.

Zhang H, Shi XQ, Hampong M, Blanis L & Pelech S (2001). Stress-induced inhibition of ERK1 and ERK2 by direct interaction with p38 MAP kinase. *J Biol Chem* **276**, 6905–6908.

Zhu YH, Mao XO, Sun YJ, Xia ZG & Greenberg DA (2002). p38 Mitogen-activated protein kinase mediates hypoxic regulation of Mdm2 and p53 in neurons. *J Biol Chem* **277**, 22909–22914.

Acknowledgements

This work was supported by the Danish National Research Council (21-01-0507 and 21-04-0535 EKH, 21-02-0120 STC), the Carlsberg Foundation (0894-10 EKH) and Novo Nordic (EKH). Dr Berthe M. Willumsen (Institute of Molecular Biology and Physiology, University of Copenhagen) and Kristine H. Beisner (Novo Nordic) are greatly acknowledged for help with making the stable cell line of Rac. The excellent technical assistance of Birthe J. Hansen is acknowledged.